Finite-size scaling study of the liquid-vapour critical point of dipolar square-well fluids

Marianela Martín-Betancourt, Jose Manuel Romero Enrique, Luis F. Rull

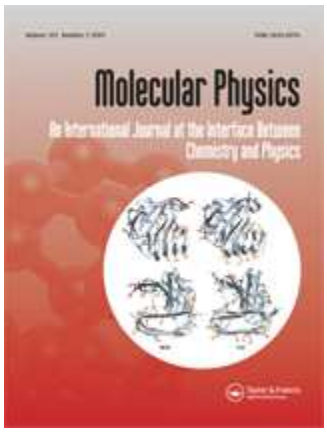

Finite-size scaling study of the liquid-vapour critical point of dipolar square-well fluids

Journal:	*Molecular Physics*
Manuscript ID:	TMPH-2009-0045.R1
Manuscript Type:	Special Issue Paper - Dr. Jean-Jacques Weis
Date Submitted by the Author:	11-Mar-2009
Complete List of Authors:	Martín-Betancourt, Marianela; Universidad de Sevilla, Departamento de Física Atómica, Molecular y Nuclear Romero Enrique, Jose Manuel; Universidad de Sevilla, Departamento de Fisica Atomica, Molecular y Nuclear Rull, Luis; Universidad de Sevilla, Departamento de Física Atómica, Molecular y Nuclear
Keywords:	Dipolar square-well fluid, Monte Carlo simulation, Liquid-vapour phase transition, Critical point, Finite-size scaling
Note: The following files were submitted by the author for peer review, but cannot be converted to PDF. You must view these files (e.g. movies) online.	
paper.tex	

Molecular Physics
Vol. 00, No. 00, Month 200x, 1–10

RESEARCH ARTICLE

Finite-size scaling study of the liquid-vapour critical point of dipolar square-well fluids

Marianela Martín-Betancourt, José Manuel Romero-Enrique and Luis F. Rull

Departamento de Física Atómica, Molecular y Nuclear, Area de Física Teórica, Universidad de Sevilla, Apartado de Correos 1065, 41080 Sevilla, Spain

(*Received 00 Month 200x; final version received 00 Month 200x*)

We present Monte Carlo simulation study in the Grand-Canonical ensemble of the liquid-vapour equilibrium of the dipolar square-well fluid for reduced dipolar moments $m^* \equiv m/\sqrt{\epsilon\sigma^3}$ in a range between 1 and $\sqrt{7}$, where ϵ is the square-well depth and σ the hard-core diameter. We locate the critical points by using the Bruce-Wilding mixed-field finite-size scaling method. In order to get the phase coexistence, we use a multiple-histogram reweighting technique. Our results are consistent with previous estimations reported in the literature, showing that the reduced critical temperature increases in terms of the square-well energy unit as the dipolar moment increases, but decreases if we take as energy unit the nose-to-tail configuration dipolar interaction. On the other hand, the critical density decreases by increasing the dipolar moment. Finally we characterize how the microscopic structure of the coexisting phases depends on the dipolar moment, paying special attention to the clustering and chain formation.

Keywords: dipolar square-well fluid, Monte Carlo simulation, liquid-vapour phase transition, critical point, finite-size scaling

1. Introduction

The fluids composed by dipolar particles has been object of extensive theoretical and simulation study in the last decades [1–3]. The presence of strong permanent electric dipolar moment changes dramatically the structural and thermodynamic properties of the dipolar fluids, and it has a deep impact in their phase diagrams. Even the simpler model of dipolar fluids (the dipolar hard-sphere system) shows a quite complex behaviour. By averaging over the orientations the dipolar interaction a Lennard-Jones-like effective potential is obtained [4, 5], so it was conjectured that the dipolar hard-sphere would have a gas-liquid phase transition similar to the observed in simple fluids. However the seminal NVT computer simulation study by Weis and Levesque [6, 7] showed no indication of a liquid-vapour transition. This result was confirmed by NPT and Gibbs ensemble simulations [8], and also observed in bidimensional and quasi-bidimensional systems [9, 10]. Furthermore the fluid structure was not the usual for simple fluids: particles formed chainlike clusters where nearest neighbour particles are in a nose-to-tail configuration. This strong chaining would interfere with the isotropic aggregation preventing the liquid-gas transition [11–15]. More recently Camp *et al* [16] reported Monte Carlo simulations which seemed to indicate a liquid-vapor phase transition in the dipolar hard sphere fluid with a reduced critical temperature $\tilde{T}_c = k_B T_c \sigma^3/m^2 \approx 0.15 - 0.16$ and reduced critical density $\rho_c^* \approx 0.1$. A mechanism for the emergence of the liquid-vapour transition was proposed by Tlusty and Safran [17]: both coexisting phases would be composed by chainlike clusters, one with a higher density of "end" defects (the

ISSN: 0040-5167 print/ISSN 1754-2278 online

DOI: 10.1080/0040516YYxxxxxxxx
http://www.informaworld.com

"vapour" phase) and another with higher density of branching points (the "liquid" phase). However, the question about the existence of liquid-vapour transition in a pure dipolar hard-sphere fluid remains unsettled.

One indirect way to confirm the existence of the liquid-vapour transition in the dipolar hard-sphere fluid is to extrapolate the behaviour of a sequence of systems which show usual vapour-liquid behaviour, but in some limit reduce to the dipolar hard-sphere model. This has been done with charged hard dumbbells [18], or by adding dispersive interactions. Different potentials for the dispersive contribution have been considered in the literature: Yukawa [19], Lennard-Jones (i.e. the Stockmayer model) [20, 21] and more recently the square-well potential [22]. As the relative strength of the dispersive interactions with respect to the dipolar forces vanishes, the dipolar hard-sphere fluid is recovered. The most studied case in the literature is the Stockmayer fluid (for a recent account of the available results, see Refs. [23, 24]). Although theoretical studies predict that the critical density vanishes in the dipolar hard-sphere limit [13, 15], the computer simulation results are not conclusive in this respect.

The main goal of this paper is to obtain accurate estimations of the critical parameters for the dipolar square-well model as the simplest dipolar fluid which takes into account dispersive forces. The liquid-vapour transition for moderate dipolar square-well fluid was already obtained by Gibbs ensemble Monte Carlo simulations in Ref. [22]. The estimation of critical parameters was done by fitting the coexistence to a power law and assuming a rectilinear diameter law. We will use more sophisticated techniques (namely finite-size scaling and multiple-histogram reweighting techniques) which are suitable for this model of dipolar fluids to obtain more precise estimations of the critical parameters, at least for moderate dipolar moments. The article is organized as follows. In Section 2 we describe the techniques used to get the critical parameters, as well as the coexistence curves. Our main results are presented in Section 3, where in addition to the discussion of the critical behaviour, we characterize the microscopic structure of the coexisting phases. Finally, we present our conclusions.

2. The model and simulation details

In the dipolar square-well fluid the particles interact through a pair potential which depends on the point dipolar moments $\vec{m}_1$ and $\vec{m}_2$ of the particles of the pair and their relative positions $\vec{r}_{12}$ as:

$$u(\vec{m}_1, \vec{m}_2, \vec{r}_{12}) = u_{SW}(r_{12}) + u_D(\vec{m}_1, \vec{m}_2, \vec{r}_{12}) \tag{1}$$

where $r_{12} = |\vec{r}_{12}|$. Thus, the total potential energy $U = \sum_{i<j} u(\vec{m}_i, \vec{m}_j, \vec{r}_{ij})$. The square-well contribution to the pair potential takes the form:

$$u_{SW}(r) = \begin{cases} \infty & r < \sigma \\ -\epsilon & \sigma < r < \lambda\sigma \\ 0 & r > \lambda\sigma \end{cases} \tag{2}$$

where σ is the hard-core diameter, which we will take as the length unit, ϵ is the square-well depth and λ defines the square-well range. As in Ref. [22], we fix the

value of $\lambda = 1.5$. The dipolar contribution has the following expression:

$$u_D(\vec{m}_1, \vec{m}_2, \vec{r}_{12}) = -\frac{m^2}{r_{12}^3}\left(3(\hat{m}_1 \cdot \hat{r}_{12})(\hat{m}_2 \cdot \hat{r}_{12}) - \hat{m}_1 \cdot \hat{m}_2\right) \quad (3)$$

where $m = |\vec{m}_1| = |\vec{m}_2|$ is the dipolar moment strength, and we define the unit vectors $\hat{m}_1 = \vec{m}_1/m$, $\hat{m}_2 = \vec{m}_2/m$ and $\hat{r}_{12} = \vec{r}_{12}/r_{12}$. Due to the dipolar contribution, the pair potential has the nose-to-tail configuration as the global minimum energy configuration.

We define the reduced dipolar moment as $m^* \equiv m/\sqrt{\epsilon\sigma^3}$. This value can be regarded as a measure of the ratio between the two relevant potential energy scales: the dipolar interaction at the nose-to-tail configuration $-2m^2/\sigma^3$, and the square-well depth $-\epsilon$. We may choose either values as energy units but, in order to compare our results with the reported in Ref. [22], we will choose ϵ as the energy length. However we may obtain the reduced energies in terms of the dipolar scale m^2/σ^3 by dividing the square-well based reduced energies by $(m^*)^2$. The reduced temperature is then defined as $T^* = k_B T/\epsilon$, where k_B is the Boltzmann constant, but we may define a dipolar-reduced temperature $\tilde{T} = k_B T\sigma^3/m^2 \equiv T^*/(m^*)^2$. We anticipate that the thermodynamic behaviour of the dipolar square-well resembles the corresponding to the pure square-well fluid in the T^* scale for $m^* \to 0$, and to the behaviour of the dipolar hard-sphere model in the $\tilde{T}$ scale for $m^* \to \infty$.

Grand-Canonical Monte Carlo (GCMC) simulations were performed using a cubic simulation box of reduced length $L^* = L/\sigma$ under periodic boundary conditions, at a reduced temperature T^* and chemical potential $\mu^* \equiv \mu/\epsilon$. In order to deal with the electrostatic interactions, we used Ewald summation technique with conducting boundary condition at infinity, with 518 Fourier-space wavevectors and real-space damping parameter $\kappa = 5$. With this choice of Ewald parameters, the relative error due to the infinite sums truncation in the electrostatic energy was shown to be less than 10^{-5} for charged systems at random configurations in small systems [25]. Other less computational intensive methods which deal with the long-range nature of the electrostatic interactions have been used in the literature, such as the Reaction Field [26] and the Wolf method [27, 28]. However, their application to systems such as charged and dipolar liquid crystals lead to equivalent results [29–31], so we expect that results will be also similar in our system. The basic steps of the simulation are attempted insertion or deletions of particles, chosen at random with the same probability. In the case of an attempted insertion, we place the particle at a random position of the box and also oriented randomly, following an uniform distribution in both cases. On the other hand, in an attempted destruction each particle has the same probability to be chosen for deletion. Usual Metropolis criterion is used to accept/reject the attempted new configuration [32]. After an initial period of equilibration, we compute the averages of the reduced total potential energy $U^* = U/\epsilon$ as well as the dipolar contribution $U_d^* = U_d/\epsilon$, and the number of particles N. The reduced density $\rho^* = \rho\sigma^3$ is defined as $\rho^* = \langle N\rangle/(L^*)^3$. In order to use the reweighting techniques, we also compute during each simulation the joint histogram of number of particles N and reduced potential energy U^*, the latter discretized in bins of width $\Delta U^* = 0.1$.

We implement the procedure to get the liquid-vapour equilibrium as described in Ref. [33]. First we locate the critical point by using a mixed-field finite-size scaling method [34] combined with a multiple-histogram reweighting technique [35]. For this purpose we run a few simulations (typically three) close to the critical point for three different sizes $L^* = 6, 8$ and 10.86. These simulations are different realizations of a simulation at the same thermodynamic conditions T^* and μ^*. Close to the crit-

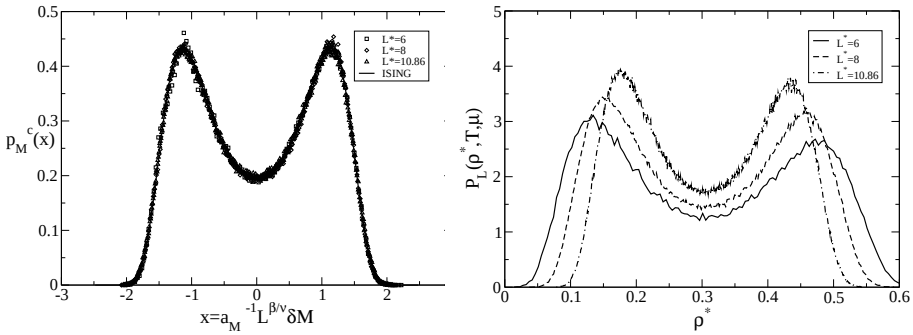

(a) (b)

Figure 1. (a): Rescaled marginal probability distributions $p^c_{\mathcal{M}}(x)$ for the dipolar square-well fluid with $\lambda = 1.5$ and $m^* = 1$. The solid line is the universal function corresponding to the 3-dimensional Ising universality class, and the symbols correspond to the best-matching simulation results: the squares correspond to $L^* = 6$, the diamonds to $L^* = 8$ and the triangles to $L^* = 10.86$. (b): Density marginal distribution function $P_L(\rho^*, T, \mu)$ for the dipolar square-well fluid with $\lambda = 1.5$ and $m^* = 2$ for the same values of temperature and chemical potential as the curves of the left panel.

ical point very long runs are needed in order to overcome the critical slowing down, so typically we performed simulations of about 10^8 GCMC steps for $L^* = 6$, 5×10^8 GCMC steps for $L^* = 8$ and 2.5×10^9 GCMC steps for $L^* = 10.86$. For each size, we combine the histograms from the different runs as shown in Ref. [35] and estimate the effective size-dependent critical parameters by minimizing the deviation of the appropriately scaled mixed-field $\mathcal{M} \propto (N - sU)/(L^*)^3$ marginal probability distribution (s is the mixing parameter) with respect to the corresponding critical 3-dimensional Ising universal function [33, 34]. Their standard errors are estimated by comparing the values obtained with the histograms corresponding to different combinations of the three runs. The dependence of the critical parameters on the simulation length L^* is due to corrections to scaling, which asymptotically behave as:

$$T_c^*(\infty) - T_c^*(L^*) \propto (L^*)^{-(1+\theta)/\nu} \qquad \rho_c^*(\infty) - \rho_c^*(L^*) \propto (L^*)^{-(1-\alpha)/\nu} \tag{4}$$

where $\alpha \approx 0.119$ and $\nu \approx 0.629$ are the Ising model critical exponents associated to the heat capacity and the correlation length, respectively, and $\theta \approx 0.54$ is the correction-to-scaling exponent. We will fit our size-dependent critical parameters to this expression in order to extrapolate the values of the critical parameters of an infinite system.

Once the critical point is located, we obtain the liquid-vapour envelope up to $\lesssim 0.98T_c$ by reweighting a histogram which combines the near-critical ones for $L^* = 8$ with other histograms obtained from shorter simulations at different thermodynamic conditions. These conditions are chosen in such a way that the combined histogram covers the relevant range of number of particles and energies for the coexisting states. At coexistence, the areas under each peak of the resulting bimodal histogram (corresponding to the vapour and liquid branches) are requested to be the same. This condition ensures pressure equality for both coexisting phases. The coexisting densities are then obtained by locating the number of particles corresponding to the two maxima of the combined histogram.

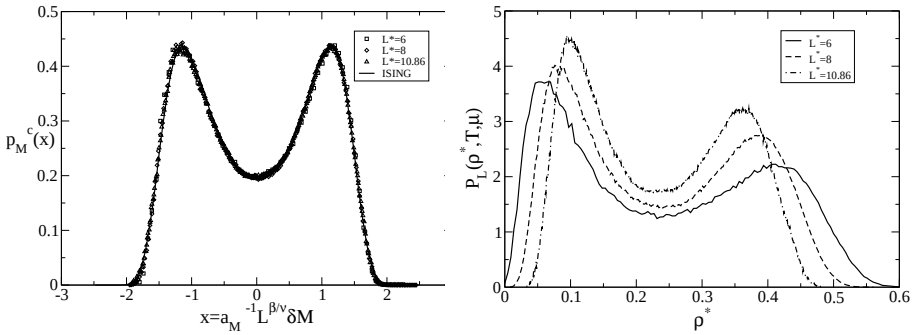

(a) (b)

Figure 2. The same as Fig.1 but for $m^* = \sqrt{7}$.

3. Results

Using the Bruce-Wilding procedure [33, 34] explained in the previous section, we have located the critical points of the dipolar square-well fluids for $(m^*)^2 = 1, 2, 3, 4, 5, 6$ and 7. As examples, we show the results of this procedure for $m^* = 1$ and $m^* = \sqrt{7}$ in Figs. 1 and 2, respectively. The left panels in both figures show the optimal matching for $L^* = 6$, 8 and 10.86 of the marginal distribution functions for the magnetization-like variable $x = a_{\mathcal{M}}^{-1}(L^*)^{\beta/\nu}(\mathcal{M} - \langle\mathcal{M}\rangle)$, being $\mathcal{M} = (N - sU)/(L^*)^3$, with the universal distribution function $P_{\mathcal{M}}^c(x)$ corresponding to the Ising universality class. We estimate the critical values of reduced temperature T_c^* and chemical potential μ_c^*, as well as the mixing parameter s, as those which minimize the deviation of the marginal distribution function with respect to the expected universal distribution. On the other hand, the value of the nonuniversal parameter $a_{\mathcal{M}}^{-1}$ is chosen in such a way that each marginal distribution has variance 1. The excellent data collapse observed for these values of m^* is a common feature of all the studied cases, although the matching is slightly better as the system is larger and/or the dipolar moment is smaller.

The density distribution function corresponding to the values of temperature and chemical potential which optimize the matching with the Ising magnetization distribution function are shown at the right panels of Figs. 1 and 2 for $m^* = 1$ and $m^* = \sqrt{7}$, respectively. As expected, they cover a large range of densities, and they become narrower as L^* increases. Two characteristics are obvious from their comparison: first the probability distributions at a given size shift towards lower values of the density as the dipolar moment increases. On the other hand, the critical distributions become more asymmetric for larger dipolar moment. Both features are observed to vary smoothly with the reduced dipolar moment m^* in the considered range.

We summarize the values of the critical parameters obtained by our matching procedure in Table 1. We confirm that the reduced temperature increases as the dipolar moment increases, but the critical density decreases. We can also see that the mixing parameter is of the same order as the reported for the pure square-well fluid $s = -0.025(4)$ [36], but it seems to decrease slightly for larger dipolar moments, in agreement with the previous observation that the density probability distributions become more asymmetric. However, the large uncertainties in the critical value of this parameter prevents us from giving a more categorical statement. After locating the critical point, we obtained the liquid-vapor coexistence curves by using the multiple-histogram reweighting technique described in the previous section. The results are shown in Fig. 3, and they are in reasonable agreement with

Table 1. Apparent critical parameters of the dipolar square-well fluid with $\lambda = 1.5$. The 1σ statistical uncertainties refer to the last decimal places.

$(m^*)^2$	L^*	T_c^*	$-\mu_c^*$	ρ_c^*	$-s$
1	6	1.309(1)	2.9799(2)	0.306(5)	0.031(4)
	8	1.311(1)	2.962(1)	0.305(2)	0.021(4)
	10.86	1.309(1)	2.971(1)	0.305(1)	0.027(5)
	∞	1.309(1)	-	0.305(1)	-
2	6	1.460(1)	3.1123(7)	0.299(5)	0.027(2)
	8	1.459(1)	3.095(1)	0.298(2)	0.028(2)
	10.86	1.460(1)	3.0906(6)	0.296(1)	0.024(5)
	∞	1.460(1)	-	0.294(1)	-
3	6	1.624(1)	3.280(3)	0.287(5)	0.033(2)
	8	1.627(3)	3.265(6)	0.286(2)	0.023(9)
	10.86	1.627(1)	3.2689(8)	0.285(1)	0.031(6)
	∞	1.628(1)	-	0.284(1)	-
4	6	1.798(4)	3.460(7)	0.275(5)	0.031(2)
	8	1.796(1)	3.488(2)	0.271(2)	0.032(2)
	10.86	1.799(1)	3.452(2)	0.272(2)	0.030(7)
	∞	1.798(3)	-	0.269(3)	-
5	6	1.968(3)	3.658(10)	0.262(5)	0.032(1)
	8	1.972(1)	3.657(2)	0.260(2)	0.031(3)
	10.86	1.971(1)	3.633(2)	0.257(1)	0.035(2)
	∞	1.973(2)	-	0.253(1)	-
6	6	2.141(1)	3.824(3)	0.251(5)	0.033(2)
	8	2.142(1)	3.881(4)	0.247(2)	0.033(1)
	10.86	2.144(2)	3.795(5)	0.247(2)	0.036(4)
	∞	2.144(1)	-	0.243(2)	-
7	6	2.313(4)	4.018(3)	0.241(5)	0.033(2)
	8	2.317(2)	3.973(6)	0.237(2)	0.033(1)
	10.86	2.319(2)	4.011(6)	0.234(2)	0.035(2)
	∞	2.321(2)	-	0.229(2)	-

the data obtained by Monte Carlo simulations in the Gibbs ensemble in Ref. [22].

Fig.4 shows the reduced temperature in terms of the dipolar energy unit and the reduced density in terms of the inverse of the squared value of the reduced dipolar moment (i.e. the reduced value of the square-well depth ϵ in the dipolar energy scale). The values of the reduced temperature for $m^* \geq 2$ are fitted quite nicely by the straight line $\tilde{T}_c = 0.1713(7) + 1.116(3)/(m^*)^2$, so the extrapolated value in the dipolar hard-sphere limit $m^* \to \infty$ is consistent with previous estimations $\tilde{T}_c \sim 0.15 - 0.16$ reported in the literature [16, 18]. On the other hand, the critical density decays much steeper than the critical temperature, so we are not able to give an extrapolation for the dipolar hard sphere critical value from our results, but in any case the values are still far away from the estimated critical density for the dipolar hard-sphere fluid. This observation indicates that the considered range for the dipolar moments is not broad enough to observe completely the crossover to the regime in which the square well contribution may be completely neglected.

Finally we characterize the change of the microscopic structure as the dipolar moment increases. For this purpose we run NVT Monte Carlo simulations with $N = 256$ for each dipolar moment at corresponding states $T = 0.9T_c$ and $\rho = \rho_c/3$ (vapour phase) and $\rho = 2\rho_c$ (liquid state). In each simulation we move and reorient each particle 10^5 times in average. The trial movement parameters are taken such to get 40%-50% as acceptance rate. From each simulation we obtain some correlation functions $h_{l_1 l_2 l}(r)$ obtained as projections of the pair distribution function on to rotational invariants [38]. We pay special attention to the function h_{112} which indicates the occurrence of nose-to-tail conformations:

$$h_{112}(r) = \frac{3\langle \sum_{i<j} \delta(r_{ij} - r)[3(\hat{m}_i \cdot \hat{r}_{ij})(\hat{m}_j \cdot \hat{r}_{ij}) - \hat{m}_i \cdot \hat{m}_j]\rangle}{4\pi N \rho^* r^2} \qquad (5)$$

Additionally we perform an analysis of the cluster formation in the vapour and the

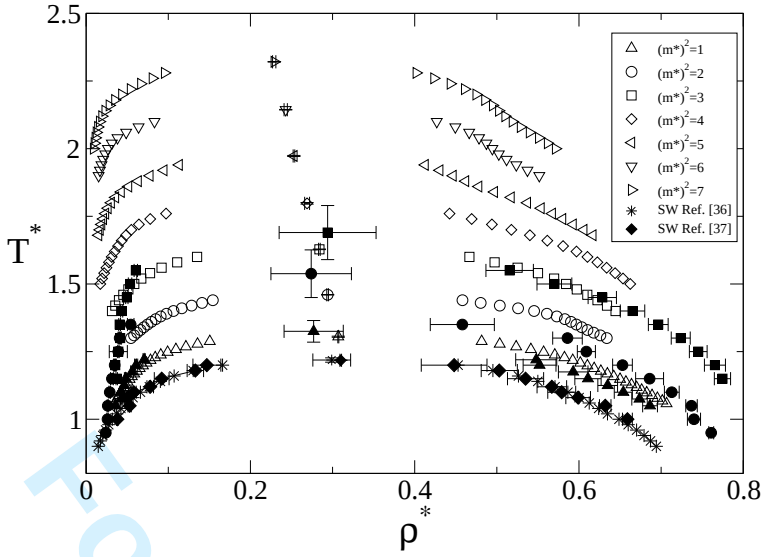

Figure 3. Liquid-vapour coexistence curves for the dipolar square well fluid for $\lambda = 1.5$ and reduced dipolar moments, from bottom to top, $m^* = 1, \sqrt{2}, \sqrt{3}, 2, \sqrt{5}, \sqrt{6}$ and $\sqrt{7}$. Open symbols correspond to our results with the multiple-histogram reweighting technique, and filled symbols correspond to the coexistence curves for $m^* = 1, \sqrt{2}$ and $\sqrt{3}$ obtained by Gibbs ensemble Monte Carlo simulations in Ref. [22]. For comparison we include the coexistence curve for the square well (SW) fluid ($m^* = 0$) obtained by the multiple histogram reweighting technique [36] (stars) and by Gibbs ensemble simulations [37] (filled diamonds).

average number of near neighbours of each particle. Two particles are considered near neighbours if the distance between their center of masses is less than some cut-off radius R_c which we take as 1.1σ. However, two near neighbours are considered to be in the same cluster if their separation is less than R_c *and* $(\hat{m}_i \cdot \hat{r}_{ij})(\hat{m}_j \cdot \hat{r}_{ij}) < R_\alpha^2$, where the angular cutoff is taken to be $R_\alpha = 0.8$. In this way we identify the chain-like clusters formed in the vapour phase. Other criteria have been proposed in the literature [15], and although the obtained results depend on the considered cutoffs, the qualitative picture is preserved.

Plots of the correlation functions h_{112} for the vapour and liquid phases are shown in Fig.5. A sudden increase (over one decade) of the value at contact $r = \sigma$ is observed in both phases as the dipolar moment changes from $m^* = 1$ to $m^* = \sqrt{7}$ (note the log scale for h_{112}). On the other hand, the function becomes more structured in both phases as a second peak at around $r \approx 2\sigma$ is already observed for $m^* = 2$ in the vapour phase (although is already present in the liquid phase for $m^* = 1$), and even a third one emerges in the vapour phase $m^* = \sqrt{7}$. The low densities involved in the vapour phase preclude a packing origin of this structure, but to the onset of chaining of the particles. This is confirmed by the peak positions (multiples of σ) and by the cluster analysis. In the left panel of Fig. 6 we plot the reduced densities of particle clusters in the vapour phase, It is clear that the population of dimers and larger clusters increases with the dipolar moment. On the other hand, the distribution of particles with N near neighbours x_N becomes flatter for small $N \leq 2$, which is another indication of the formation of chains. However even for $m^* = \sqrt{7}$ most of the particles are isolated. Larger dipolar moments m^* are needed to observe chaining in the near-critical vapour phase.

4. Conclusions

In this paper we have done a GCMC simulation study of the liquid-vapour criticality and coexistence of the dipolar square-well potential. We have obtained accurate

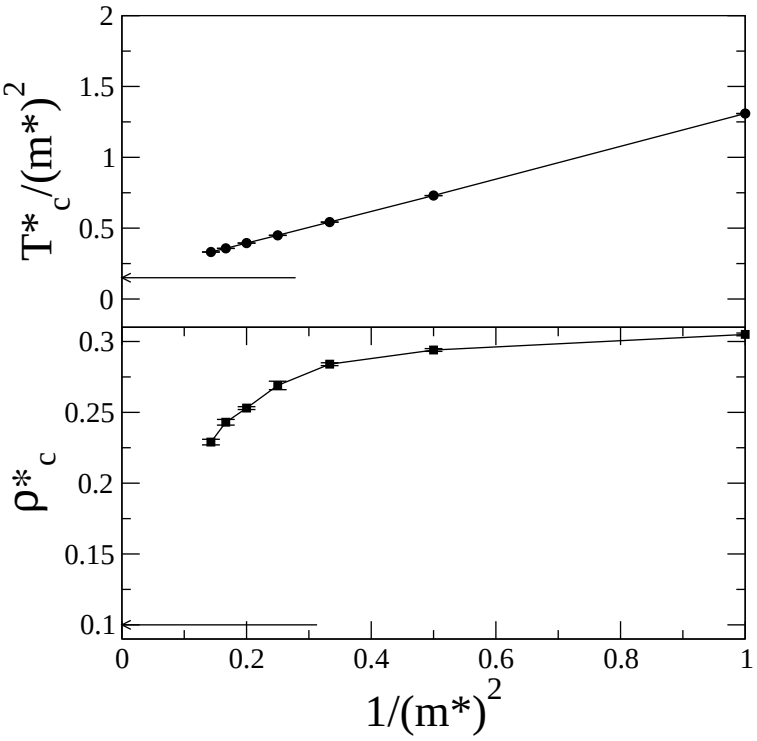

Figure 4. Plot of the dipolar-reduced critical temperature $\tilde{T}_c$ (upper panel) and the reduced temperature ρ_c^* (lower panel) as a function of $(m^*)^{-2}$. The arrows indicate the previous estimations of the critical temperature and density for the dipolar hard sphere fluid [16, 18]. The lines which join the data points are only for eye guide.

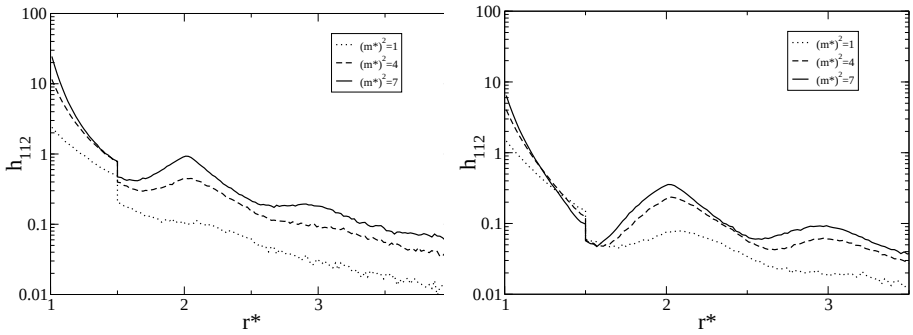

Figure 5. (a): Plot of the correlation function h_{112} at the vapour phase in a corresponding state $T = 0.9T_c$ and $\rho = \rho_c/3$ for $m^* = 1$ (dotted line), $m^* = 2$ (dashed line) and $m^* = \sqrt{7}$ (continuous line). (b): Plot of the correlation function h_{112} at the liquid phase in a corresponding state $T = 0.9T_c$ and $\rho = 2\rho_c$. The meaning of the symbols is the same as in the left panel.

estimations of the critical parameters by using multiple-histogram reweighting and mixed-field finite-size scaling methods. Additionally we have obtained the coexistence curves and characterized the microscopic structure of the coexisting phases. Although the temperature has the expected trend with the dipolar moment and its extrapolation to the dipolar hard-sphere case is consistent with previous estimations, the obtained values of critical density are still far from the predicted value for the dipolar hard-sphere fluid. This observation, together with the low clustering observed in the vapour phase even for $m^* = \sqrt{7}$, shows that the considered range of dipolar moments is not broad enough to crossover to the regime where

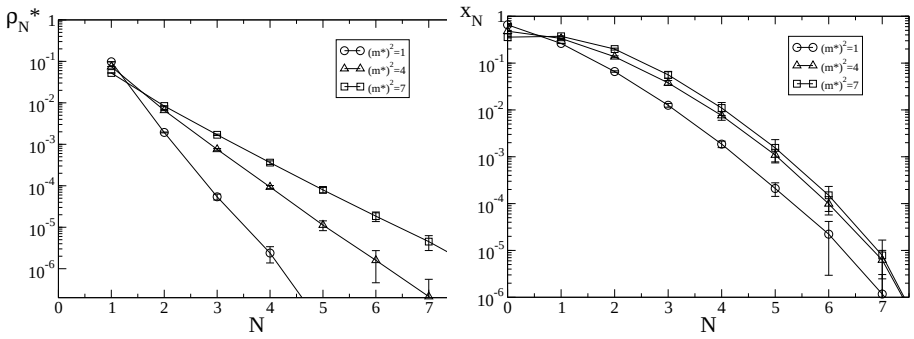

Figure 6. (a): Plot of reduced cluster densities $\rho_N^* \equiv \rho_N \sigma^3$ as a function of the number of particles N which compose them, for $m^* = 1$ (circles), $m^* = 2$ (triangles) and $m^* = \sqrt{7}$ (squares). The lines are only for eye guide. (b): Plot of fraction of particles x_N with N near neighbours. The meaning of the symbols is the same as in the left panel.

the dispersive interactions can be neglected. This can be rationalized by the fact that close to criticality and for the larger considered dipolar moment the reduced value of the square-well depth (in terms of the dipolar energy unit) $\tilde{\epsilon} = 1/(m^*)^2$ is of the same order as the thermal energy $\tilde{T} \sim T_c^*/(m^*)^2$, although both are smaller than unity. This fact suggests we should continue for larger values of m^* to get faithful extrapolations of the critical parameters in the dipolar hard-sphere model. As the acceptance rate is lowered when we increase the dipolar moment, we anticipate that we will need configurational bias techniques in order to get results with the same accuracy as the considered in this paper. This issue is beyond the scope of this paper, and further work is needed in that direction to solve convincingly the question of whether the dipolar hard-sphere model has liquid-vapour phase transition or not.

Acknowledgments

The authors would like to thank Dr. G. Orkoulas for providing us the coexistence curve data of the $\lambda = 1.5$ square-well fluid from Ref.[36]. We acknowledge the finantial support of Ministerio de Ciencia y Tecnología (Spain) through Grant VEM2003-20574-C03-02, Ministerio de Educación y Ciencia (Spain) through Grant ENE2007-68040-C03-02, and Junta de Andalucía through "Plan Andaluz de Investigación" (Group FQM-205).

References

[1] J.-J. Weis and D. Levesque, Adv. Polym. Sci. **185**, 163 (2005).
[2] P.I.C. Teixeira, J.M. Tavares and M.M. Telo da Gama, J. Phys.: Condens. Matter **12**, R411 (2000).
[3] B. Huke and M. Lücke, Rep. Prog. Phys. **67**, 1731 (2004).
[4] C.E. Woodward and S. Nordholm, Molec. Phys. **52**, 973 (1984).
[5] P. Frodl, B. Groh and S. Dietrich, Ber. Bunsenges. Phys. Chem. **98**, 503 (1994).
[6] J.J. Weis and D. Levesque, Phys. Rev. Lett. **71**, 2729 (1993).
[7] D. Levesque and J.J. Weis, Phys. Rev. E **49**, 5131 (1994).
[8] J.M. Caillol, J. Chem. Phys. **98**, 9835 (1993).
[9] J.J. Weis, Molec. Phys. **93**, 361 (1998).
[10] A. Gil-Villegas, S.C. McGrother and G. Jackson, Chem. Phys. Lett. **269**, 441 (1997).
[11] R. P. Sears, Phys. Rev. Lett. **76**, 2310 (1996).
[12] R. van Roij, Phys. Rev. Lett. **76**, 3348 (1996).
[13] J.M. Tavares, M.M. Telo da Gama and M.A. Osipov, Phys. Rev. E **56**, R6252 (1997).
[14] Y. Levin, Phys. Rev. Lett. **83**, 1159 (1999).
[15] J.M. Tavares, J.J. Weis and M.M. Telo da Gama, Phys. Rev. E **59**, 4388 (1999).

[16] P.J. Camp, J.C. Shelley and G.N. Patey, Phys. Rev. Lett. **84**, 115 (2000).
[17] T. Tlusty and S.A. Safran, Science **290**, 1328 (2000).
[18] G. Ganzenmüller and P.J. Camp, J. Chem. Phys. **126**, 191104 (2007).
[19] I. Szalai, D. Henderson, D. Boda and K.-Y. Chan, J. Chem. Phys. **111**, 337 (1999).
[20] M.E. van Leeuwen and B. Smit, Phys. Rev. Lett. **71**, 3991 (1993).
[21] M.J. Stevens and G.S. Grest, Phys. Rev. E **51**, 5976 (1995).
[22] A.L. Benavides, S. Lago, B. Garzón, L.F. Rull and F. del Río, Molec. Phys. **103**, 3243 (2005).
[23] A.O. Ivanov, S.S. Kantorovich and P.J. Camp, Phys. Rev. E **77**, 013501 (2008).
[24] R. Hentschke and J. Bartke, Phys. Rev. E **77**, 013502 (2008).
[25] G. Hummer, Chem. Phys. Lett. **235**, 297 (1995).
[26] J. A. Barker and R. O. Watts, Molec. Phys. **26**, 789 (1973).
[27] D. Wolf, Phys. Rev. Lett. **68**, 3315 (1992).
[28] D. Wolf, P. Keblinnski, S.R. Phillpot and J. Eggebrecht, J. Chem. Phys. **110**, 8254 (1999).
[29] A. Gil-Villegas, S. C. McGrother and G. Jackson, Molec. Phys. **92**, 723 (1997).
[30] M. Houssa, L. F. Rull and S. C. McGrother, J. Chem. Phys. **109**, 9529 (1998).
[31] C. Avedaño and A. Gill-Villegas, Molec. Phys. **104**, 1475 (2006).
[32] D. Frenkel and B. Smit, *Understanding Molecular Simulations: From Algorithms to Applications* 2nd ed. (Academic Press, San Diego, 2002).
[33] A.Z. Panagiotopoulos, J. Phys.: Condens. Matter **12**, R25 (2000).
[34] N.B. Wilding and A.D. Bruce, J. Phys.: Condens. Matter **4**, 3087 (1992).
[35] A.M. Ferrenberg and R.H. Swendsen, Phys. Rev. Lett. **61**, 2635 (1988); *ibid.* **63**, 1195 (1989).
[36] G. Orkoulas and A.Z. Panagiotopoulos, J. Chem. Phys. **110**, 1581 (1999).
[37] L. Vega, E. de Miguel, L. F. Rull, G. Jackson and I. A. McLure, J. Chem. Phys. **96**, 2296 (1992).
[38] C.G. Gray and K.E. Gubbins, *Theory of Molecular Fluids. Volume 1: Fundamentals* (Clarendon Press, Oxford, 1984).